

Transistor Device Optimization for RF Power Amplifier Employing Rapid Envelope Load-Pull System

Mohammad S. Hashmi*, Paul J. Tasker**, and Fadhel M. Ghannouchi*

*iRadio Lab, Schulich School of Engineering, University of Calgary, T2N1N4, Canada

Tel: 1-403-210-7941, E-mail: mshashmi@ucalgary.ca

**Center for HF Engineering, School of Engineering, Cardiff University, CF243AA, U. K.

Tel: 44-29-20876347; E-mail: Tasker@cf.ac.uk

Abstract— This paper reports mathematical explanation and the application domain of rapid envelope load-pull system. It is demonstrated that this novel load-pull technique finds immediate use in the optimization of transistor devices for the design of microwave power amplifiers. The limitations of the existing load-pull systems severely affect the overall performance optimization of transistor devices. The envelope load-pull improves on the limitations of the existing systems and thus provides a very effective methodology for the design and investigation of the RF power amplifiers. Initially the paper describes the mathematical foundation of the envelope load-pull concept and then the rapid, accurate and reliable measurement capability of the system is presented. It clearly vindicates the potential areas of application of the system in improving the measurement throughput and yield optimization of the microwave devices. Finally, the harmonic envelope load-pull is utilized on a commercially available 1W GaAs FET that demonstrates the rapid RF power amplifier design, investigation and optimization strategy.

Index Terms— Envelope Load-pull, Harmonic Load-pull, Microwave Measurements, Microwave Power Amplifier, Transistor Device Optimization.

I. INTRODUCTION

Large signal RF device characterization is a critical component in the design and optimization process of a power amplifier (PA). Through the use of load-pull the device can be subjected to the impedance environments required for the design and optimization of PAs. The procedures such as load-pull, also called load tuning mechanism,

characterizations are extensively conducted on transistor devices for the determination of optimum matching conditions at the input and output port of the microwave device. Traditionally various methods of load-pull utilizing passive and active techniques are employed for the synthesis of desired load at the device input or output terminals.

The classical approach of load synthesis employs passive techniques [1-3]. However the inherent losses, in the network between the device under test (DUT) and the tuner, prevent the system from obtaining reflection coefficient closer to the edge of Smith chart. It has been demonstrated in [4] that the optimizations of transistor devices for higher efficiency PAs require termination of harmonic impedances at open or short conditions, and thus limiting the usefulness of the passive techniques in these investigations.

To overcome the limitations of the passive systems, active load-pull approaches are utilized where emulation of load impedance is achieved by injecting an amplified signal of specific magnitude and phase into the DUT output. Such active systems can have either an “open loop” or “closed loop” architecture. In a “closed loop” system, presented in [5], the injected signal is a modified version (direct function) of the DUT output signal. This ensures that the emulated load impedance is independent of drive level and thus is fast. But unfortunately, due to closed loop architecture, this approach is prone to RF oscillations.

In the alternative “open loop” system, reported in [6-7], the injected signal is generated independently. This system is free from oscillations but requires iterative convergence to synthesize and maintain constant load. This results in a slow load emulation process and hence finds limited applicability in designs where harmonic contributions are significant or where designs require rapid yield and turnaround in the PA design and optimization process.

It is thus evident that the optimum load-pull system should exhibit the advantages of all the existing load-pull techniques. The authors reported a concept of an emerging load-pull technique in [8] that exhibits the useful features of all the existing load-pull approaches and termed it as Envelope Load Pull (ELP). Recently reported results in [9] also prove that the ELP can synthesize loads at different harmonics which are independent of each other.

This paper gives the mathematical description of the ELP system and then demonstrates that the rapid load emulation capability of this technique is extremely useful in developing strategy for optimizing the microwave devices for PA applications.

II. POWER AMPLIFIER DESIGN CHALLENGE

The power amplifier is an extremely critical component in many microwave systems. Its performance decides the overall power consumption, robustness and size of the entire system. The power dissipation in the PA must be minimized at the optimum input power levels for achieving the best efficiencies and this imposes a very strict challenge for the power amplifier designers. However, the amplifier design challenge is complex, since the device non-linear behavior must be accounted for as the active device is operating under large signal conditions. To fully account for these non-linear effects or exploit them in the design process, ideally the power amplifier designer would like to know

how the setting of specific parameters affects the overall performance of the device as quickly as possible. Existing systems are capable of providing this information, but these systems take a significant amount of measurement time. Thus one of the requirements is to speed up the measurement systems to expedite the overall design process.

In summary, the amplifier designers face extremely difficult trade-off among the contrasting goals of high transmitted power, low power consumption and even for many telecommunication systems linear operation. Hence, critical to this requirement is a suitable measurement system that can aid in understanding the performance of the active device under different operating conditions in a short time frame.

This paper presents the mathematical foundation of the setup reported in [9-10] and briefly discusses the realization of the measurement system. Then an experimental investigation is reported in this paper that underlines the usefulness of this ELP based measurement setup in the development of rapid and accurate strategy for the design and optimization of PAs.

III. MATHEMATICAL EXPLANATION OF ENVELOPE LOAD-PULL SYSTEM

The concept, design and calibration methodologies of ELP technique have been reported in [8-10]. This section aims to present the mathematical explanation of the design strategy of the ELP system. The Fig. 1 presents the pictorial explanation of the mathematical process taking place in the ‘ELP Module’.

The main components of ‘ELP Module’ are IQ-demodulator, ‘control unit’ and IQ-modulator. The IQ-demodulator down converts the input signal, b_2 , to the baseband components I_b and Q_b that are modified appropriately in the ‘control unit’ by external control variables, X and Y, to formulate I_a and Q_a .

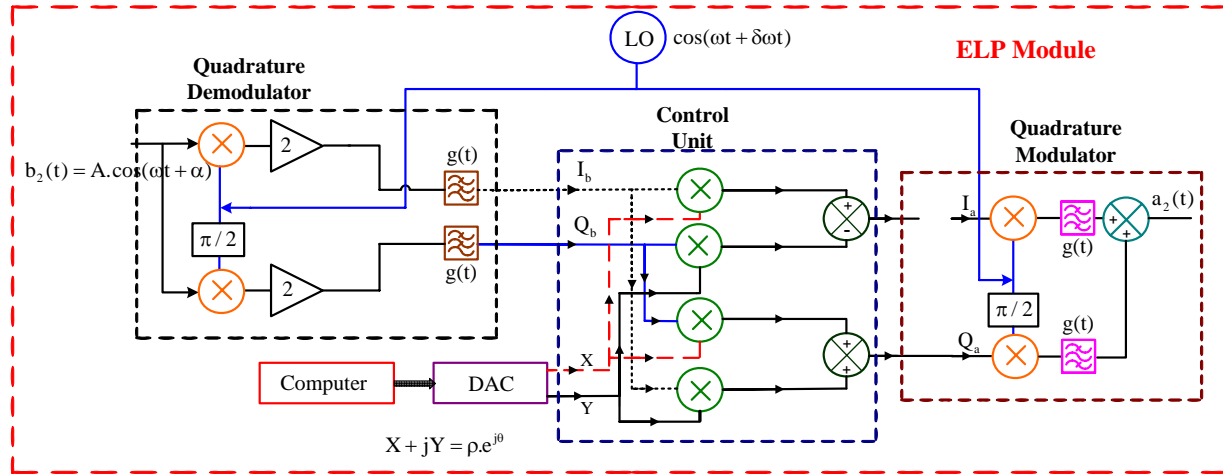


Fig. 1. Block Diagram Explaining the Operation of Envelope Load-Pull Module

The IQ-modulator up converts the modified baseband components I_a and Q_a with the use of coherent local oscillator (LO) to form the output signal, a_2 . The emulated load reflection coefficient is given by:

$$\Gamma_{load} = \frac{a_2}{b_2} \quad (1)$$

Hence the output signal, a_2 , must satisfy the following condition:

$$a_2 = \Gamma_{load} \cdot b_2 \quad (2)$$

The equivalent envelope domain expression is given by:

$$I_a(t) + jQ_a(t) = \Gamma_{load} \cdot (I_b(t) + jQ_b(t)) \quad (3)$$

In equation 3, $I_a(t) + jQ_a(t)$ and $I_b(t) + jQ_b(t)$ represent the base band components of a_2 and b_2 signals respectively. In this system the desired load reflection coefficient, Γ_{load} is set by the control unit given by:

$$\Gamma_{load} = X + jY = \rho \cdot e^{j\theta} \quad (4)$$

Where $\rho = \sqrt{X^2 + Y^2}$ and $\theta = \tan^{-1}(Y / X)$ represent the magnitude and phase of the desired

load respectively, obtained by the control of external signals X and Y . The complete mathematical explanation of this load emulation mechanism in the ELP system is explained below.

Assuming that the signal, $b_2(t)$, received by the demodulator is co-sinusoidal with an amplitude (A) and a phase (α) operating at a frequency of (ω) and the demodulator is operating with a LO frequency of ($\omega + \delta\omega$) then:

$$b_2(t) = A \cos(\omega t + \alpha) = \frac{A}{2} (e^{j(\omega t + \alpha)} + e^{-j(\omega t + \alpha)}) \quad (5)$$

The quadrature demodulator down-converts this signal into baseband components given in equation (6) and (7).

$$I_b(t) = 2 \cdot \{A \cos(\omega t + \alpha) \cos(\omega t + \delta\omega t)\} \quad (6)$$

$$Q_b(t) = 2 \cdot \{A \cos(\omega t + \alpha) \sin(\omega t + \delta\omega t)\} \quad (7)$$

The scaling factor of 2 in (6) and (7) accounts for the losses in the demodulator. For simplification purposes, the following parameters are defined:

$$K = e^{j\omega t}; m = e^{j\alpha}; p = e^{j\delta\omega t}; \quad (8)$$

Hence equation (6) can be re-written using (8) to:

$$I_b(t) = \frac{A}{2} \left(K_m + \frac{1}{K_m} \right) \cdot \left(K_p + \frac{1}{K_p} \right) \quad (9)$$

$$I_b(t) = A \left\{ \frac{1}{2} \left(\frac{p}{m} + \frac{m}{p} \right) + \frac{1}{2} \left(K^2 m p + \frac{1}{K^2 m p} \right) \right\} \quad (10)$$

If the terms including K^2 which are harmonic components of the local oscillator frequency are removed by the filter function of the demodulator, $g(t)$, then:

$$I_b(t) = A \left\{ \frac{1}{2} \left(\frac{p}{m} + \frac{m}{p} \right) \right\} = A \cdot \cos(\delta\omega t - \alpha) \quad (11)$$

The same process when applied to (7) gives the following the result:

$$Q_b(t) = A \cdot \sin(\delta\omega t - \alpha) \quad (12)$$

It can be seen that time domain I and Q Signals in (11) and (12) map out a circle on the complex plane where the starting angle of the circle is $-\alpha$. Combining (11) and (12) into their complex form and then using (3) for load emulation at the envelope frequency results into:

$$E_{b2}(t) = A \cdot \{ \cos(\delta\omega t - \alpha) + j \sin(\delta\omega t - \alpha) \} = A \cdot e^{j(\delta\omega t - \alpha)} \quad (13)$$

$$E_{a2}(t) = E_{b2}(t) \cdot \Gamma_{Load} = E_{b2}(t) \cdot \rho \cdot e^{j\theta} = A \cdot \rho \cdot e^{j(\delta\omega t - \alpha + \theta)} \quad (14)$$

Now, E_{a2} from (14) can be written in complex form as:

$$E_{a2}(t) = A \cdot \rho \{ \cos(\delta\omega t - \alpha + \theta) + j \sin(\delta\omega t - \alpha + \theta) \} \quad (15)$$

Up-converting E_{a2} using the same quadrature LO of frequency $(\omega + \delta\omega)$ gives:

$$a_2(t) = A \cdot \rho \{ \{ \cos(\delta\omega t - \alpha + \theta) \cos(\omega t + \delta\omega t) \} + \{ \sin(\delta\omega t - \alpha + \theta) \sin(\omega t + \delta\omega t) \} \} \quad (16)$$

The following parameter, d , given in equation (17), is defined for the simplification of equation (16).

$$d = e^{j\theta} \quad (17)$$

Then the expansion of equation (16) results in:

$$a_2(t) = \frac{A\rho}{4} \left\{ 2 \left(\frac{Kmp}{pd} + \frac{pd}{Kmp} \right) + \frac{Kp^2d}{m} + \frac{m}{Kp^2d} - \frac{Kp^2d}{m} - \frac{m}{Kp^2d} \right\} \quad (18)$$

If the terms including K^2 which are harmonic components are removed by the filter function of the modulator, $g(t)$, then:

$$a_2(t) = A \cdot \rho \cdot \cos(\omega t + \alpha - \theta) \quad (19)$$

Comparing (19) with (5) shows that mathematically the phase and frequency of the RF input signal is preserved when passing through the 'ELP Module', but the output magnitude and phase can be altered, by changing the values of ρ and θ respectively, by controlling X and Y. The load presented to the device at frequency ω is then the ratio of the Fourier transform of equation (19) divided by the Fourier transform of equation (5) evaluated at ω :

$$\Gamma_{Load}(\omega) = \frac{F\{A\rho\cos(\omega t + \alpha - \theta)\}}{F\{A\cos(\omega t + \alpha)\}} = \rho \cdot \frac{e^{-j(\alpha - \theta)}}{e^{-j(\alpha)}} = \rho \cdot e^{j\theta} \quad (20)$$

The equation (20) defines the load reflection coefficient emulated by active envelope load-pull and exactly matches equation (4).

IV. REALIZATION OF THE ENVELOPE LOAD-PULL SYSTEM

The configuration of the realized active harmonic ELP system is given in Fig. 2. It utilizes commercially available IQ-demodulator, quadrature multipliers to implement control unit and IQ-modulated ESG to provide an ELP module for one harmonic loop. Three harmonic

setups require three sets of these components. The utilized ESG also provides a coherent carrier as a local oscillator for the IQ-demodulator. The circulator isolates the ESG from any reflections occurring at the triplexer ports. The directional coupler isolates the injected signal, a_2 , from the transmitted signal, b_2 .

In the case of fundamental frequency, the up-converted signal coming out of the ESG is the injected signal, a_2 , which emulates the required load reflection coefficient, Γ_{Load} , at the reference plane for a particular harmonic as defined by equation (1). The desired load reflection coefficient for other harmonics can be similarly obtained by controlling the respective harmonic ‘ELP Module’.

The harmonic ELP system is then integrated into the time domain measurement setup reported in [11] and shown in Fig. 3, providing a fully functional 3-harmonic load-pull system for power amplifier design optimization.

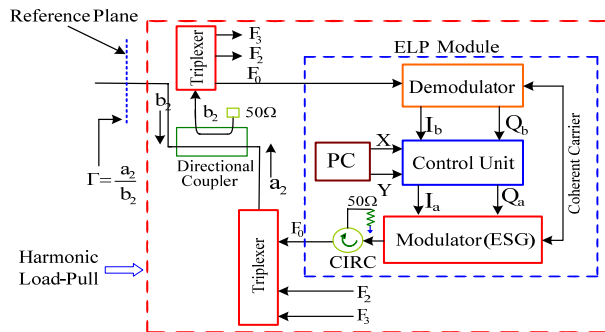


Fig.2. Configuration of the realized multi-harmonic ELP System

The system employs a 2-channel Microwave Transition Analyzer (MTA) as receiver for measuring the four traveling waves a_1 , b_1 , then a_2 and b_2 . One data point capture of all the travelling waves using the MTA generally takes under 30 seconds, which is now the critical time element within device characterization measurements as it will be shown, the rapid load setting feature of ELP removes the load setting

bottleneck. The speed of measurements, could be further increased by employing a 4-channel sampling oscilloscope that could capture all four travelling waves in a single measurement, without the need to diplex the signals.

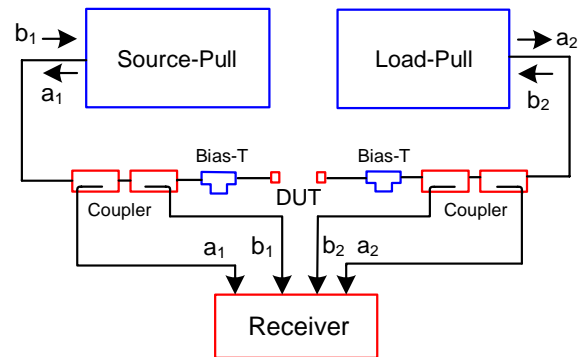


Fig.3. Block Diagram of the Time Domain Measurement System

V. EVALUATION OF THE SYSTEM

The first step in the deployment of the harmonic ELP is the calibration of each ELP module so that the user is able to set the desired load properly. Accordingly the calibration for each module is performed at the desired frequency level as explained in [9-10]. In this case the fundamental ELP was calibrated at 850 MHz and the second and third harmonic ELP were calibrated at 1.7 GHz and 2.5 GHz respectively.

It has been reported in [9-10] that the ELP system is capable of setting the desired load reflection coefficients in a rapid manner and the respective load reflection coefficients at different harmonic frequencies are independent of each other. To demonstrate and utilize these properties of the system, a 1W GaAs FET (model-FLL107ME) from Fujitsu at the fundamental frequency of 850 MHz and biased in class-AB is employed for the demonstration of rapid emulation of fundamental and harmonic load impedances.

A. Rapid load emulation at fundamental frequency

For the determination of optimal fundamental loading condition a sweep over 4x4 impedance grid was performed around the possible fundamental optimal impedance, identified from the datasheet. Then the achieved load-pull contour is derived over the impedance grid for fundamental output power as given in Fig. 4. During this measurement the second and third harmonic impedances were actively held at 50Ω respectively.

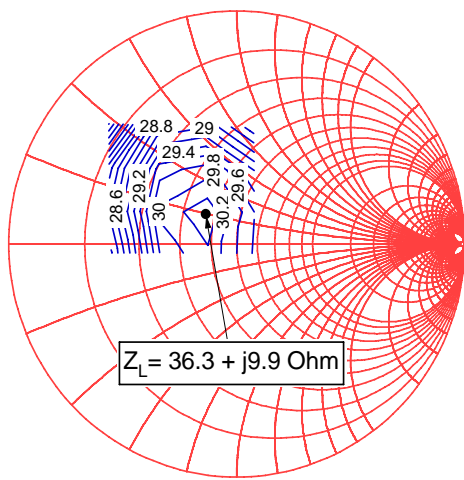


Fig.4. Measured load-pull fundamental power contour on the 4x4 impedance grid

It is evident from the measured load-pull contour that the optimal output power is 30.2 dBm. It is similar to that mentioned in the device datasheet. The corresponding optimal fundamental impedance, $Z_{opt}(F_0)$, for maximum output power as obtained from the load-pull contour is found to be $36.3 + j9.9\Omega$. The rapid load emulation characteristic of the ELP system allows this whole measurement of 16 impedance point to be carried out in less than 7 minutes. This shorter time frame of optimal impedance determination using the ELP system is a quite significant improvement over the existing passive and active load-pull systems.

B. Determination of second harmonic impedance

This investigation requires the application of rapid load setting as well as the harmonically independent load emulation features of the ELP system. To determine the optimal second harmonic impedance, first the fundamental impedance is fixed at the identified fundamental optimal value, $Z_{opt}(F_0) = 36.3 + j9.9\Omega$. Then the second harmonic impedance is swept over a 12x12 impedance grid while keeping the third harmonic impedance actively matched to 50Ω. The result of this measurement is displayed in Fig. 5. It is evident that the fundamental and third harmonic impedances are unchanged during the 144 points second harmonic impedance and thereby vindicating that indeed the harmonic impedances are independent of each other.

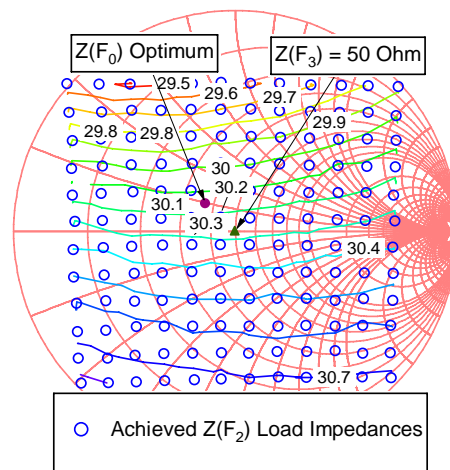


Fig.5. Measured $Z(F_2)$ impedances and the respective fundamental load-pull contour over the 12x12 grid

It is apparent from load-pull contour given in Fig. 5 that the power output from the device shows a progressing trend in the third and fourth quadrant of the Smith chart and thus clearly identifying that the second harmonic impedance is located somewhere near the bottom edge of the Smith chart. Therefore another appropriate second harmonic impedance grid of 6x4 is swept near the bottom edge of Smith chart to find out its optimal value. The achieved result from this measurement is displayed in Fig. 6 which clearly identifies that indeed the second harmonic

impedance lies near the border of Smith chart. The optimal second harmonic impedance, $Z_{opt}(F_2)$, is determined from this measurement data which comes out to be $0.011-j1.053\Omega$. It is clear that the output power from this device when the fundamental and second harmonic is set at their respective optimal values is 30.84 dBm. The total time required to carry out the measurement on 168 impedance points for the determination of optimal second harmonic impedance is under 75 minutes.

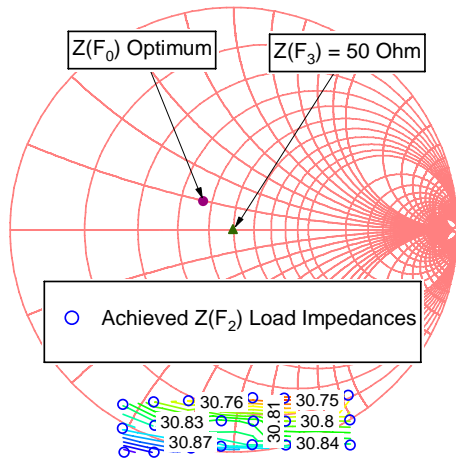


Fig.6. Measured $Z(F_2)$ impedances and the respective fundamental load-pull contour over the 6x4 grid

C. Determination of second harmonic impedance

For the determination of third harmonic impedance, the fundamental is set at $Z_{opt}(F_0)$ whereas the second harmonic impedance is actively set at 50Ω . Then a sweep over a third harmonic impedance grid of 12x12 is carried out and the corresponding output power contour is extracted from this impedance sweep. The achieved impedance points and the output power contour are shown in Fig. 7.

The output power shows a progressive nature in the first quadrant and this necessitate a further measurement on 4x4 third harmonic impedance grid near the border of the Smith chart in the first

quadrant. The resulting third harmonic impedances $Z(F_3)$ and the corresponding output power contour is given in Fig. 8.

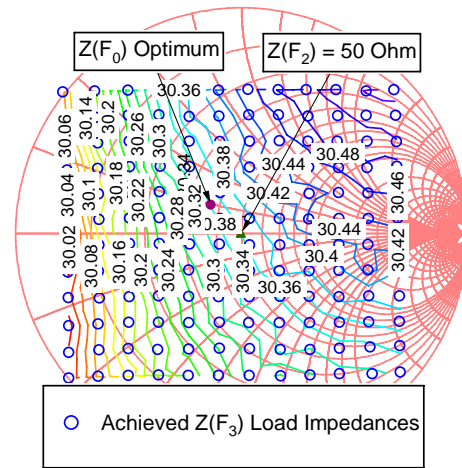


Fig.7. Measured $Z(F_3)$ impedances and the respective fundamental load-pull contour over the 12x12 grid

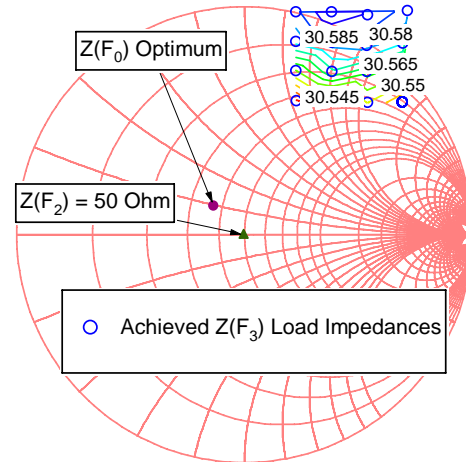


Fig.8. Measured $Z(F_3)$ impedances and the respective fundamental load-pull contour over the 4x4 grid

The optimal third harmonic impedance, $Z_{opt}(F_3)$, can be easily identified from this investigation and the value of which comes out to be $1.3 + j100\Omega$. The output power when the fundamental and third harmonic impedances are held at their respective optimal is 30.585 dBm.

The accurate identification of fundamental, second harmonic and third harmonic optimal impedances require measurements on 344 impedance points. This whole investigation takes just under 2.5 hours which is a substantial saving in the measurement time. The existing active and passive load-pull is either slow or cannot synthesize harmonically independent load impedances. The ELP technique thus significantly speeds up the measurement time and is a very effective tool, in the rapid PA design, characterization and optimization process, and hence finds immediate application in speeding up the time-to-market of microwave devices and circuits.

VI. RAPID DEVICE OPTIMIZATION

To demonstrate the rapid optimization process of microwave device for Power Amplifier application, the earlier identified optimal load impedances for 1W GaAs FET at fundamental, $Z_{opt}(F_0)$, second harmonic, $Z_{opt}(F_2)$, and third harmonic, $Z_{opt}(F_3)$, are utilized. The device is biased in class-AB mode and the fundamental impedance is set at its optimal value of $36.3 + j9.9\Omega$ for all the investigation discussed in this section.

Initially power sweeps are conducted for two different conditions while actively holding the third harmonic impedance, $Z(F_3)$, to 50Ω . In the first case, the measurements are conducted for the case where the second harmonic termination is held at $Z_{opt}(F_2)$, while in the second case the $Z(F_2)$ is actively held at 50Ω . The obtained drain efficiency and gain results are displayed in Fig. 9. It is evident that the appropriate termination of second harmonic improves the drain efficiency by more than 5% and also advances the output power at 1dB compression by 2 dB.

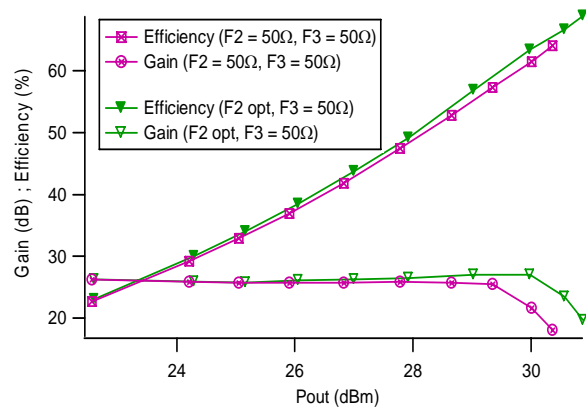


Fig.9. Comparing power sweep plots for second harmonic at 50Ω and $Z_{opt}(F_2)$

In the second investigation, the $Z(F_2)$ is actively held at 50Ω and the measurements are conducted for the cases where the third harmonic termination is held firstly at $Z_{opt}(F_3)$ and then actively held at 50Ω . The obtained drain efficiency and gain results are given in Fig. 10. It is apparent that the appropriate termination of the third harmonic impedance can have an impact on the linear gain, increasing the output power at 1dB compression by 1.5 dB. For this device, the impact of optimal third harmonic impedance on the drain efficiency is minimal as the improvement is only 2%.

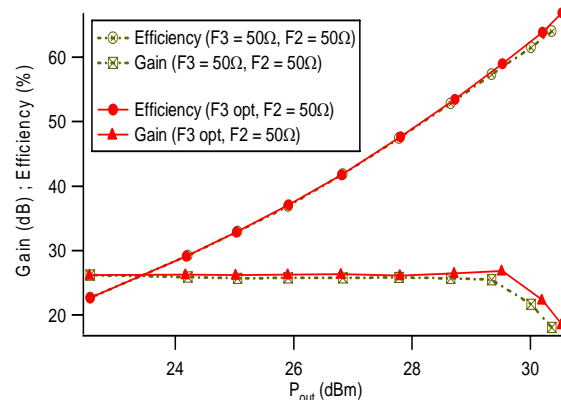


Fig.10. Comparing power sweep plots for third harmonic at 50Ω and $Z_{opt}(F_3)$

Finally the second and third harmonics are held at their respective optimal load impedances and



the measurements are carried out. The plot in Fig. 11 displays the achieved drain efficiency and gain results when the fundamental, second and third harmonic are held to their respective optimal values. It is evident that, for this specific device, the optimal second and third harmonic terminations produce overall increase of 7% in the drain efficiency and increase of around 2.5dB in the output power at 1dB compression point.

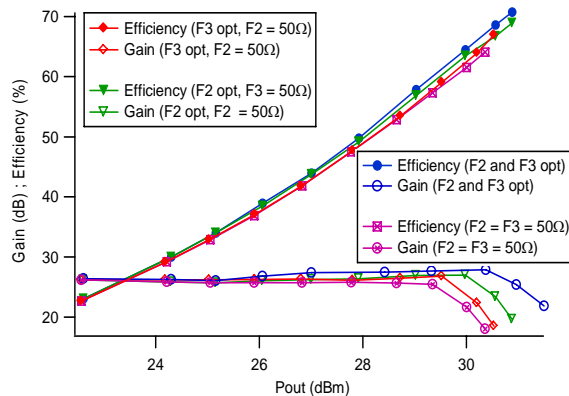


Fig.11. Comparing power sweep plots for $Z_{opt}(F_2)$ and $Z_{opt}(F_3)$ independently with power sweep plots with fundamental at $Z_{opt}(F_0)$

This whole device optimization process, involving measurements of 40 data points in total, took less than 20 minutes of measurement time which was achieved due to the fact that the harmonic load impedances once set are independent of drive power and independent from each other; therefore no further iterations are required to present the correct impedances. The measurement time could be further reduced by deploying 4-channel receiver for capturing the measurement data. This will save the time spent on switching between the receiver channels.

This type of accurate and reliable optimization is not possible to carry out in such a short time frame using active open-loop load-pull [12] as measurement of one data point using this system requires around 6 minutes and thereby requiring 240 minutes for the overall measurements. The traditional passive load-pull system is limited in

this type of device optimization technique, due to two main factors: a) the inability to set accurate harmonically independent load impedance, and b) the inability to set harmonic load impedances near the border of Smith chart, and thereby is unsuited for such applications.

VII. CONCLUSION

This paper provided the complete mathematical concept behind the operation of the ELP system. It has been explained through mathematical treatment of the system that the phase and frequency of the RF input signal is preserved when passing through the 'ELP Module', but the output magnitude and phase can be altered, by changing the values of ρ and θ respectively, by controlling external control variables X and Y. It is thus evident that the system is very simple to design and operate and has potential to replace or augment the existing active open-loop load-pull and passive load-pull systems.

This paper has also outlined the application of the ELP system in the rapid optimization of microwave devices for PA application. The ELP system is able to instantly achieve load impedances at the available harmonics anywhere on the Smith chart and even beyond, which are also independent of drive power, bias and other harmonics. As demonstrated with a commercially available device, these unique properties of the ELP system readily lends itself for new, previously unviable load-pull measurements of devices; enabling a measurement-driven PA design and optimization process.

ACKNOWLEDGEMENT

The authors would like to acknowledge the helps of Mr. Alan Clarke and Dr. Jonathan Lees of Center for High Frequency Engineering, Cardiff University. The authors thank Dr. Steve Cripps for interesting discussions on RFLPA design and characterization.

REFERENCES

- [1] R. B. Stancliff and D. P. Poulin, "Harmonic load-pull", *MTT-S International Microwave Symposium*, Florida, USA, pp. 185-187, April 30 - May 2, 1979.
- [2] Maury Microwave Corporation, "Device Characterization with Harmonic Load and Source Pull", *Application Note: 5C-044*, Dec. 2000.
- [3] Focus Microwave, "Load Pull Measurements on Transistors with Harmonic Impedance Control", *Technical Note*, August 1999.
- [4] C. Roff, J. Benedikt and P. J. Tasker, "Design approach for realization of very high efficiency power amplifiers", *IEEE MTT-S International Microwave Symposium*, Hawaii, USA, pp. 143-146, June 3-8, 2007.
- [5] G.P. Bava, U. Pisani, V. Pozzolo, "Active Load Technique for Load-Pull Characterisation at Microwave Frequencies" *Electronic Letters*, Vol. 18, No. 4, pp. 178-180, Feb. 1982.
- [6] Y. Takayama, "A New load-Pull Characterization Method for Microwave Power Transistors", *IEEE MTT-S international Microwave Symposium*, New Jersey, USA, pp. 218-220, June 14-16, 1976.
- [7] J. Benedikt, R. Gaddi, P. J. Tasker, M. Goss, "High-power Time-domain Measurement System with Active Harmonic Load-pull for High-efficiency Base-station Amplifier Design", *IEEE Trans. Microwave Theory Tech.*, Vol. 48, Issue 12, pp. 2617-2624, Dec. 2000.
- [8] T. Williams, J. Benedikt, P. J. Tasker, "Experimental Evaluation of an Active Envelope Load-Pull Architecture for High Speed Device Characterization," *IEEE MTT-S international Microwave Symposium*, Long Beach, USA, pp. 1509-1512, June 12-17, 2005.
- [9] M. S. Hashmi, A. L. Clarke, S. P. Woodington, J. Lees, J. Benedikt and P. J. Tasker, "Electronic Multi-harmonic Load-pull System for Experimentally Driven Power Amplifier Design Optimization", *IEEE MTT-S International Microwave Symposium*, Boston, USA, pp. 1549-1552, June 6-12, 2009.
- [10] M. S. Hashmi, A. L. Clarke, S. P. Woodington, J. Lees, J. Benedikt and P. J. Tasker, "An Accurate Calibrate-able Multi-Harmonic Active Load-Pull System based on the Envelope Load-Pull Concept", *IEEE Trans. Microwave Theory Tech.*, Vol. 3, Issue 3, pp. 656-664, March 2010.
- [11] D. Williams and P. J. Tasker, "An Automated Active Source and Load Pull Measurement System", *6th IEEE High Frequency Student Colloquium*, Dublin, Ireland, pp. 7-12, Sept. 9-10, 2001.
- [12] Mueller, J. E.; Gyselinckx, B.; "Comparison of Active versus Passive On-Wafer Load-Pull Characterization of Microwave MM-Wave Power Devices", *IEEE MTT-S international Microwave Symposium*, San Diego, USA, pp. 1077-1080, May 23-27, 1994.